

RESEARCH

Open Access



# Second-order TGV model for Poisson noise image restoration

Hou-biao Li\*, Jun-yan Wang and Hong-xia Dou

\*Correspondence:  
lihoubiao0189@163.com  
School of Mathematical  
Sciences, University  
of Electronic Science  
and Technology of China,  
Chengdu 611731, People's  
Republic of China

## Abstract

Restoring Poissonian noise images have drawn a lot of attention in recent years. There are many regularization methods to solve this problem and one of the most famous methods is the total variation model. In this paper, by adding a quadratic regularization on TGV regularization part, a new image restoration model is proposed based on second-order total generalized variation regularization. Then the split Bregman iteration algorithm was used to solve this new model. The experimental results show that the proposed model and algorithm can deal with Poisson image restoration problem well. What's more, the restoration model performance is significantly improved both in visual effect and objective evaluation indexes.

**Keywords:** Image restoration, Poisson noise, Total generalized variation, Split Bregman iteration, Optimization problem

## Background

Image restoration is a fundamental and unavoidable problem in digital image processing by reconstructing the blurred or noisy image from the observed image and not losing the details of image (Zhao et al. 2013; Bilal et al. 2015). There are abundant methods to restore these images. For example, in Zhao et al. (2013), a Bayesian minimum mean squared error (MMSE) estimation based on high-order non-local range-Markov random field (NLRMRF) prior is proposed for non-blind image deblurring problem. The constrained optimization framework (Bilal et al. 2015) was presented to solve the image spatial degradation problem. Moreover, an adaptive weighted regularization scheme was also proposed in modified error estimate (MEE) to cater with the uncertainty due to ill-posed nature of the inverse problem in Bilal et al. (2015). In terms of regularization models, one of the most remarkable models was the ROF model introduced by Rudin et al. (1992), which presented total variation regularization for removing the additive Gaussian white noise. The total variation (TV) model assumed the original image  $u$  to be defined on  $\Omega \subset \mathbb{R}^2$  and obtained a solution from a minimization problem

$$F(u) := \int_{\Omega} |\nabla u| + \frac{\lambda}{2} \int_{\Omega} |f - u|^2, \quad (1)$$

where the first term is the total variation regularization term, the second term is fidelity term and  $\lambda$  is a positive fidelity parameter. Although the TV model is effective in image processing, specially for Gaussian white noise. However, this model is not effective in restoring Poisson noise images such as astronomical (Starck and Murtagh 2007), biomedical (Dey et al. 2006; Sarder and Nehorai 2006; Willett and Nowak 2003), and photographic imaging (Foi et al. 2005). For this reason, scholars have proposed some new methods to deal with Poisson noise image problems.

Le et al. (2007) proposed a new total variation model to recover image corrupted by Poisson noise, the new total variation model with fidelity term is suitable for Poisson noise. The new model can be written as

$$\min_u \int_{\Omega} |Du| + \lambda \int_{\Omega} (Ku - f \log Ku). \quad (2)$$

The authors used the gradient descent method to obtain its optimum solution. However, this method can not obtain optimal approximation when the image is both high intensity noise and low intensity features. In Sawatzky et al. (2013), an efficient EM-TV algorithm is presented to speed the computation of the optimization problem (2). In addition, alternating split Bregman iterative algorithm (Setzer et al. 2010) is also used to solve the question (2), since this algorithm does not contain iterations and also not produce negative values. In addition, Figueiredo and Bioucas-Dias (2010) proposed an approach based on alternating direction optimization method for deconvolving Poissonian images.

Recently, based on Chavent and Kunisch (1997) and Liu and Huang (2012) proposed another new total bounded variation-based Poissonian images restoration model

$$\min_u \int_{\Omega} |Du| + \frac{\lambda_1}{2} \|u\|^2 + \lambda_2 \int_{\Omega} (Ku - f \log Ku). \quad (3)$$

Although the above model is better than the total variation model and has a competitive superiority, there also exist some shortcomings, for example, sometimes it will cause undesired oil painting artifacts. In order to avoid the staircase effect, many methods have been proposed. A well-known method to eliminate staircase effect is the TGV (Bredies et al. 2010; Bredies and Valkonen 2011; Bredies et al. 2013) regularization. The TGV regularizer can effectively eliminate the staircase effect but there are still some shortcomings, it tends to introduce some blurring on image edges and texture regions as the existence of high-order derivative term. More seriously, some small details will be lost during the denoising. For this reason, we consider combine the TGV and  $\|u\|^2$  as one regularization term to solve the poisson noise image restoration problem.

The rest of this article is organized as follows. In “Total generalized variation (TGV)” section, we briefly review the total generalized variation (TGV). The proposed model and algorithm are presented in “The proposed Poisson noise recovering model and algorithm” section. In “Experimental results and discussions” section, experimental results are illustrated to show the consistent performance of the proposed method. Finally, conclusions are given in “Conclusions” section.

### Total generalized variation (TGV)

Bredies et al. (2010) proposed the concept of total generalized variation (TGV), which is considered to be the generalization of TV. For convenience, some concepts of TGV are given as follows.

**Definition 1** (Bredies et al. 2010) Let  $\Omega \subset \mathbb{R}^d$  be a domain,  $k \geq 1$  and  $\alpha = (\alpha_0, \dots, \alpha_{k-1}) > 0$ . Then, the total generalized variation of order  $k$  with weight  $\alpha$  for  $u \in L^1_{loc}(\Omega)$  is defined as the value of the function

$$TGV_{\alpha}^k(u) = \sup \left\{ \int_{\Omega} u \operatorname{div}^k v \, dx \mid v \in C_c^k(\Omega, \operatorname{Sym}^k(\mathbb{R}^d)), \right. \\ \left. \|\operatorname{div}^l v\|_{\infty} \leq \alpha_l, \quad l = 0, \dots, k-1 \right\}, \quad (4)$$

where  $\operatorname{Sym}^k(\mathbb{R}^d)$  denotes the space of symmetric tensors of order  $k$  with arguments in  $\mathbb{R}^d$ , and  $\alpha_l$  are fixed positive parameters.

**Definition 2** (Bredies et al. 2010) The space of bounded generalized variation is defined as

$$BGV_{\alpha}^k(\Omega) = \left\{ u \in L^1(\Omega) \mid TGV_{\alpha}^k(u) < \infty \right\}, \\ \|u\|_{BGV_{\alpha}^k} = \|u\|_1 + TGV_{\alpha}^k(u). \quad (5)$$

Here  $BGV_{\alpha}^k(\Omega)$  is a Banach space independent of the weight vector  $\alpha$ .

**Definition 3** (Bredies et al. 2010) The “dualization” in the definition of the functional  $TGV_{\alpha}^k$  can also be informally interpreted in terms of iterated Fenchel duality.

$$TGV_{\alpha}^k(u) = \inf_{\substack{u_l \in C^{k-l}(\Omega, \operatorname{Sym}^l(\mathbb{R}^d)) \\ l=1, \dots, k-1, u_0=u, u_k=0}} \sum_{l=1}^k \alpha_{k-l} \|\varepsilon(u_{l-1}) - u_l\|_1. \quad (6)$$

Note that the tensor field  $u_l$  are in different spaces for varying  $l$ . Moreover, the operator  $\varepsilon(u_{l-1})$  denotes the symmetrized gradient operator

$$\varepsilon(u_{l-1}) = \frac{\nabla u_{l-1} + (\nabla u_{l-1})^T}{2}. \quad (7)$$

In this paper, we use  $k = 2$  in the proposed model. Thus, the second-order TGV can be written as

$$TGV_{\alpha}^2(u) = \sup \left\{ \int_{\Omega} u \operatorname{div}^2 w \, dx \mid w \in C_c^2(\Omega, S^{d \times d}), \|w\|_{\infty} \leq \alpha_0, \|\operatorname{div} w\|_{\infty} \leq \alpha_1 \right\}, \quad (8)$$

where  $S^{d \times d}$  denotes the space of symmetric  $d \times d$  matrices. And the first and second divergences are defined as

$$(\operatorname{div} w)_h = \sum_{j=1}^d \frac{\partial w_{hj}}{\partial x_j}, \quad 1 \leq h \leq d, \quad (9)$$

$$\operatorname{div}^2 w = \sum_{h,j=1}^d \frac{\partial^2 w_{hj}}{\partial x_h \partial x_j}. \quad (10)$$

In addition, according to Bredies and Valkonen (2011), the energy term  $TGV_\alpha^2$  can be formulated as

$$TGV_\alpha^2 = \min_{u \in BGV_\alpha^2(\Omega), p \in BD(\Omega)} \alpha_1 \int_\Omega |\nabla u - p| + \alpha_0 \int_\Omega |\varepsilon(p)|, \quad (11)$$

where  $\varepsilon(p)$  can be separately expressed as

$$\varepsilon(p) = \begin{bmatrix} \nabla_x p_1 & \frac{1}{2}(\nabla_y p_1 + \nabla_x p_2) \\ \frac{1}{2}(\nabla_y p_1 + \nabla_x p_2) & \nabla_y p_2 \end{bmatrix}. \quad (12)$$

### The proposed Poisson noise recovering model and algorithm

#### The proposed model for Poisson noise image

We assume that  $u \in \mathbb{R}_+^N$  is the original image,  $f \in \mathbb{R}^N$  is the observed image,  $K \in \mathbb{R}^{N \times N}$  is a linear blurring operator related with the spread point function (PSF). Then the degradation model can be described as

$$f = P(Ku), \quad (13)$$

where  $P$  denotes the Poisson distribution function.

Based on Le et al. (2007), we define the Bayes Law as follows.

$$P(u|f) = \frac{P(f|u)P(u)}{P(f)}. \quad (14)$$

According to (14), for each  $u \in \Omega$ , we have

$$P(f|Ku) = \prod_{i=1}^N P(f_i|(Ku)_i) = \prod_{i=1}^N \frac{e^{-(Ku)_i} ((Ku)_i)^{f_i}}{f_i!}. \quad (15)$$

Next, we assume that the prior distribution  $P(u)$  is TGV and  $\|u\|^2$ , which can be written as

$$p(u) = \exp \left( -\frac{\lambda}{2} \|u\|_2^2 - TGV_\alpha^2 \right), \quad (16)$$

where  $\lambda$  is the regularization parameter.

Thus, we obtain a model for restoring the Poissonian noise image as follows.

$$\min_u \beta \sum_{i=1}^N (Ku)_i - f_i \log (Ku)_i + \frac{\lambda}{2} \|u\|_2^2 + TGV_\alpha^2 + l_{\mathbb{R}^+}(u), \quad (17)$$

where  $l_s$  is the indicator function of set  $S$

$$l_S(u) = \begin{cases} 0, & \Leftarrow u \in S; \\ +\infty, & \Leftarrow u \notin S. \end{cases} \quad (18)$$

$$u_+ = \max \{0, u\}, \quad \log(0) = -\infty, \quad \text{and} \quad 0 \log(0) = 0.$$

By reformulating TGV as a minimization in the discrete setting, the proposed model can be written as

$$\begin{aligned} \min_u \beta \int_{\Omega} (Ku - f \log(Ku)) dx + \frac{\lambda}{2} \|u\|_2^2 + \alpha_1 \|\nabla u - p\|_1 \\ + \alpha_0 \|\varepsilon(p)\|_1 + l_{\mathbb{R}^+}(u). \end{aligned} \quad (19)$$

### The split Bregman algorithm for Poisson noise removal

The split Bregman algorithm (Goldstein and Osher 2009; Wang et al. 2008) has been widely used in image processing, which is easy to be realized and has fast convergence (Cai et al. 2009; Jia et al. 2009). Therefore, we use split Bregman algorithm to solve our minimization problem (19). Firstly, by introducing new auxiliary variables  $w$ ,  $x$ ,  $y$  and  $z$ , the problem (19) can be reformulated as the following constrained optimization problem

$$\begin{aligned} \min_u \beta \int_{\Omega} w - f \log w + \frac{\lambda}{2} \|u\|_2^2 + \alpha_1 \|x\|_1 + \alpha_0 \|y\|_1 + l_{\mathbb{R}^+}(z) \\ \text{s.t. } Ku = w, \quad \nabla u - p = x, \quad \varepsilon(p) = y, \quad u = z. \end{aligned} \quad (20)$$

For the above constrained problem (20), we transform it into the corresponding unconstrained problem

$$\begin{aligned} \min_u \beta \int_{\Omega} w - f \log w + \frac{\lambda}{2} \|u\|_2^2 + \alpha_1 \|x\|_1 + \alpha_0 \|y\|_1 \\ + l_{\mathbb{R}^+}(z) + \frac{\mu_1}{2} \|Ku - w\|_2^2 + \frac{\mu_2}{2} \|\nabla u - p - x\|_2^2 \\ + \frac{\mu_3}{2} \|\varepsilon(p) - y\|_2^2 + \frac{\mu_4}{2} \|u - z\|_2^2, \end{aligned} \quad (21)$$

where  $\mu_i (i = 1, \dots, 4)$  are positive penalty parameters. Thus the split Bregma iterative algorithm for solving the question (20) can be described as

$$\begin{aligned} (w^{k+1}, x^{k+1}, y^{k+1}, z^{k+1}, u^{k+1}, p^{k+1}) = \min_u \beta \int_{\Omega} w - f \log w \\ + \frac{\lambda}{2} \|u\|_2^2 + \alpha_1 \|x\|_1 + \alpha_0 \|y\|_1 + l_{\mathbb{R}^+}(z) + \frac{\mu_1}{2} \|Ku - w - b_1^k\|_2^2 \\ + \frac{\mu_2}{2} \|\nabla u - p - x - b_2^k\|_2^2 + \frac{\mu_3}{2} \|\varepsilon(p) - y - b_3^k\|_2^2 \\ + \frac{\mu_4}{2} \|u - z - b_4^k\|_2^2, \end{aligned} \quad (22)$$

where the updates of the multipliers  $b_1, b_2, b_3, b_4$  is described as follows

$$\begin{aligned} b_1^{k+1} &= b_1^k + (Ku^{k+1} - w^{k+1}); \\ b_2^{k+1} &= b_2^k + (\nabla u^{k+1} - p^{k+1} - x^{k+1}); \\ b_3^{k+1} &= b_3^k + (\varepsilon(p^{k+1}) - y^{k+1}); \\ b_4^{k+1} &= b_4^k + (u^{k+1} - z^{k+1}). \end{aligned} \quad (23)$$

Since the updates of  $b_1^k, b_2^k, b_3^k, b_4^k$  are merely simple calculations, then the minimization question (22) can be divided into the following several subproblems: Given initial value

$b_1^0 = b_2^0 = b_3^0 = b_4^0 = 0$  and  $u^0 = p^0 = w^0 = x^0 = y^0 = z^0 = 0$ , the split Bregman algorithm can be written as

$$\begin{cases} w^{k+1} = \arg \min_w \beta \int_{\Omega} w - f \log w + \frac{\mu_1}{2} \|Ku^k - w - b_1^k\|_2^2, \\ x^{k+1} = \arg \min_x \alpha_1 \|x\|_1 + \frac{\mu_2}{2} \|Du^k - p^k - x - b_2^k\|_2^2, \\ y^{k+1} = \arg \min_y \alpha_0 \|y\|_1 + \frac{\mu_3}{2} \|\varepsilon(p^k) - y - b_3^k\|_2^2, \\ z^{k+1} = \max \{u^{k+1} + b_4^k, 0\}, \\ (u^{k+1}, p^{k+1}) = \arg \min_{u,p} \frac{\lambda}{2} \|u\|_2^2 + \frac{\beta\mu_1}{2} \|Ku - w^{k+1} - b_1^k\|_2^2 \\ + \frac{\alpha_1\mu_2}{2} \|Du - p - x^{k+1} - b_2^k\|_2^2 + \frac{\mu_4}{2} \|u - z^{k+1} - b_4^k\|_2^2 \\ + \frac{\alpha_0\mu_3}{2} \|\varepsilon(p) - y^{k+1} - b_3^k\|_2^2. \end{cases} \quad (24)$$

For  $w$ -subproblem, note that it is separable with respect to each component. It is easy to solve and the solution of  $w$  may be written as

$$w^{k+1} = \frac{1}{2} \left( \left( Ku^k + b_1^k - \frac{\beta}{\mu_1} \right) + \sqrt{\left( Ku^k + b_1^k - \frac{\beta}{\mu_1} \right)^2 + \frac{4\beta f}{\mu_1}} \right). \quad (25)$$

As for solving  $x$ ,  $y$ -subproblem, we can directly obtain the solutions by using shrinkage operator:

The  $x$ -subproblem can be solved by

$$x^{k+1} = \max \left( \left( \|Du^k - p^k - b_2^k\|_2 - \frac{\alpha_1}{\mu_2}, 0 \right) \frac{Du^k - p^k - b_2^k}{\|Du^k - p^k - b_2^k\|_2} \right). \quad (26)$$

The solution of the  $y$ -subproblem is similarly obtained

$$y^{k+1} = \max \left( \left( \|\varepsilon(p^k) - b_3^k\|_2 - \frac{\alpha_0}{\mu_3}, 0 \right) \frac{\varepsilon(p^k) - b_3^k}{\|\varepsilon(p^k) - b_3^k\|_2} \right). \quad (27)$$

The  $(u, p)$ -subproblem is a saddle-point problem, which can be divided into the following two subproblems:

1. For  $u$ , we have

$$\begin{aligned} u^{k+1} = \arg \min_u \frac{\lambda}{2} \|u\|_2^2 + \frac{\beta\mu_1}{2} \|Ku - w^{k+1} - b_1^k\|_2^2 \\ + \frac{\alpha_1\mu_2}{2} \|Du - p - x^{k+1} - b_2^k\|_2^2 + \frac{\mu_4}{2} \|u - z^{k+1} - b_4^k\|_2^2, \end{aligned} \quad (28)$$

which can be solved by considering the following normal equation

$$\begin{aligned} \lambda u + \alpha_1 \mu_2 \sum_{j=1}^2 D_j^T (D_j u - p_j - x_j^{k+1} - b_{2j}^k) \\ + \beta \mu_1 K^T (Ku - w^{k+1} - b_1^k) + \mu_4 (u - z^{k+1} - b_4^k) = 0. \end{aligned} \quad (29)$$

Finally,  $u$  is solved by

$$\begin{aligned} u^{k+1} = \left( \lambda I + \beta \mu_1 K^T K + \alpha_1 \mu_2 \sum_{j=1}^2 D_j^T D_j + \mu_4 I \right)^{-1} \\ \times \left( \beta \mu_1 K^T (w^{k+1} + b_1^k) + \alpha_1 \mu_2 \sum_{j=1}^2 D_j^T (p_j + x_j^{k+1} + b_{2j}^k) \right. \\ \left. + \mu_4 (z^{k+1} + b_4^k) \right). \end{aligned}$$

2. For the sub-problem  $p$ , it can be written as the following minimization problem

$$\begin{aligned} p^{k+1} = \arg \min_p \frac{\alpha_1 \mu_2}{2} \|Du - p - x^{k+1} - b_2^k\|_2^2 \\ + \frac{\alpha_0 \mu_3}{2} \|\varepsilon(p) - y^{k+1} - b_3^k\|_2^2, \end{aligned} \quad (30)$$

where  $p = (p_1, p_2)^T$  is a  $2 \times 1$  vector,  $\varepsilon(p)$  is a  $2 \times 2$  matrix.

For  $p_1$ , it can be solved by considering the following linear system

$$\begin{aligned} \alpha_1 \mu_2 (p_1 - D_1 u + x_1^{k+1} + b_{21}^k) + \alpha_0 \mu_3 D_1^T (D_1 p_1 - y_1^{k+1} - b_{31}^k) \\ + \frac{\alpha_0 \mu_3}{2} D_2^T (D_2 p_1 + D_1 p_2 - 2y_3^{k+1} - 2b_{33}^k) = 0. \end{aligned} \quad (31)$$

Therefore,

$$\begin{aligned} p_1^{k+1} = (\alpha_1 \mu_2 I + \alpha_0 \mu_3 D_1^T D_1 + \frac{\alpha_0 \mu_3}{2} D_2^T D_2)^{-1} \\ \times (\alpha_1 \mu_2 (D_1 u - x_1^{k+1} - b_{21}^k) + \alpha_0 \mu_3 D_1^T (y_1^{k+1} + b_{31}^k) \\ + \frac{\alpha_0 \mu_3}{2} D_2^T (2y_3^{k+1} + 2b_{33}^k - D_1 p_2)). \end{aligned} \quad (32)$$

Similarly, we can obtain the solution of  $p_2$  as

$$\begin{aligned} p_2^{k+1} = \left( \alpha_1 \mu_2 I + \alpha_0 \mu_3 D_2^T D_2 + \frac{\alpha_0 \mu_3}{2} D_1^T D_1 \right)^{-1} \\ \times \alpha_1 \mu_2 (D_2 u - x_2^{k+1} - b_{23}^k) + \alpha_0 \mu_3 D_2^T (y_2^{k+1} + b_{32}^k) \\ + \frac{\alpha_0 \mu_3}{2} D_1^T (2y_3^{k+1} + 2b_{33}^k - D_2 p_1). \end{aligned} \quad (33)$$

## Experimental results and discussions

In this section, we illustrate some numerical results of the proposed model for the Poisson noise removal problem. We compare our method with the one proposed in Figueiredo and Bioucas-Dias (2010) (PIDAL) and the other proposed in Liu and Huang (2012) (PID-Split). In order to prove the superiority of the proposed model, we compare our model with TGV regularization model. To show the effectivity of the proposed model, we choose four pictures possessed abundant detail information.

We terminate the iterations for these methods by the following stopping criterion

$$\frac{\|u^{k+1} - u^k\|_2}{\|u^k\|_2} \leq 1 \times 10^{-3}. \quad (34)$$

The quality of the restoration results is compared quantitatively by using the Signal-to-Noise Ratio (SNR), the Peak Signal-to-Noise (PSNR), the relative error (RelErr) and the Structural SIMilarity index (SSIM). They are defined as follows

$$\text{RelErr} = \frac{\|u - \hat{u}\|_2}{\|u\|^2}, \quad \text{SNR} = 20 \log_{10} \left( \frac{\|u\|_2}{\|\hat{u} - u\|_2} \right), \quad (35)$$

$$\text{MSE} = \frac{1}{|\Omega|} \int_{\Omega} (\hat{u} - u)^2 dx, \quad \text{PSNR} = 10 \log_{10} \left( \frac{255^2}{\text{MSE}} \right), \quad (36)$$

where  $u$  and  $\hat{u}$  are the ideal image and the restored image, respectively.

$$\text{SSIM} = \frac{(2\mu_u \mu_{\hat{u}} + C_1)(2\sigma_{u\hat{u}} + C_2)}{(\mu_u^2 + \mu_{\hat{u}}^2 + C_1)(\sigma_u^2 + \sigma_{\hat{u}}^2 + C_2)}, \quad (37)$$

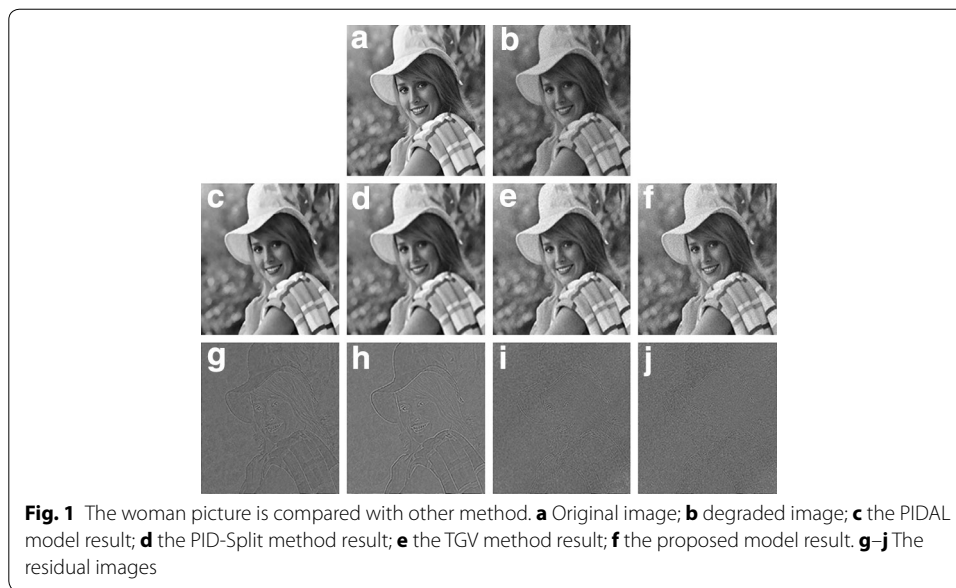
where  $\mu_u$  and  $\mu_{\hat{u}}$  are averages of  $u$  and  $\hat{u}$ , respectively.  $\sigma_u$  and  $\sigma_{\hat{u}}$  are the variance of  $u$  and  $\hat{u}$ , respectively.  $\sigma_{u\hat{u}}$  is the covariance of  $u$  and  $\hat{u}$ . The positive constants  $C_1$  and  $C_2$  can be thought of as stabilizing constants for near-zero denominator values. Generally speaking, the more bigger value of SNR, PSNR or the smaller value of RelErr is, the better quality of the reconstructed image is.

The Poissonian images used for our experiments are generated as follows: the original images are convoluted with a blur kernel and additionally contaminated by Poisson noise, here we use the **poissrnd** function in MATLAB's Statistics Toolbox after blurring the true images with the given point spread functions to generate the blurred and noise images.

The selection of the regularization parameters highly affects the image restoration results, and related to make the fair comparison with different denoising models. The penalty parameters  $\mu$  which relies on unknown noise level highly influences the speed of the algorithms. In experiments, we set  $\mu = [0.01, 0.001]$  in the PIDAL algorithm. In the PID-Split algorithms, we choose  $\mu = [0.0004; 0.1, 0.0001]$ . In the TGV model, we set  $\mu = [0.1; 10, 5, 3]$ . The penalty parameter in the proposed method is empirically set  $\mu = [0.1; 0.6; 0.1; 0.02]$ . Thus, we may have a good restoration results.

In the first experiment, we used the image "Woman" ( $512 \times 512$ ) in Fig. 1a. We perform the blurring operation  $\text{psfGauss}(5, 2)$  proposed in Nagy et al. (2004) on the original image and add the Poisson noise to the blurred data to generate the degraded image in Fig. 1b. The parameter of this test, we set  $\beta = 120$  in PIDAL algorithm,  $\beta = 6, \lambda = 0.01$  for PID-Split algorithms, due to the TGV model we set  $\beta = 450, \alpha = [8, 10]$ , set  $\beta = 54, \lambda = 0.001, \alpha = [16, 9]$  for the proposed model. The pictures of Fig. 1c-f are the restoration images, which represent the difference between the three methods. From



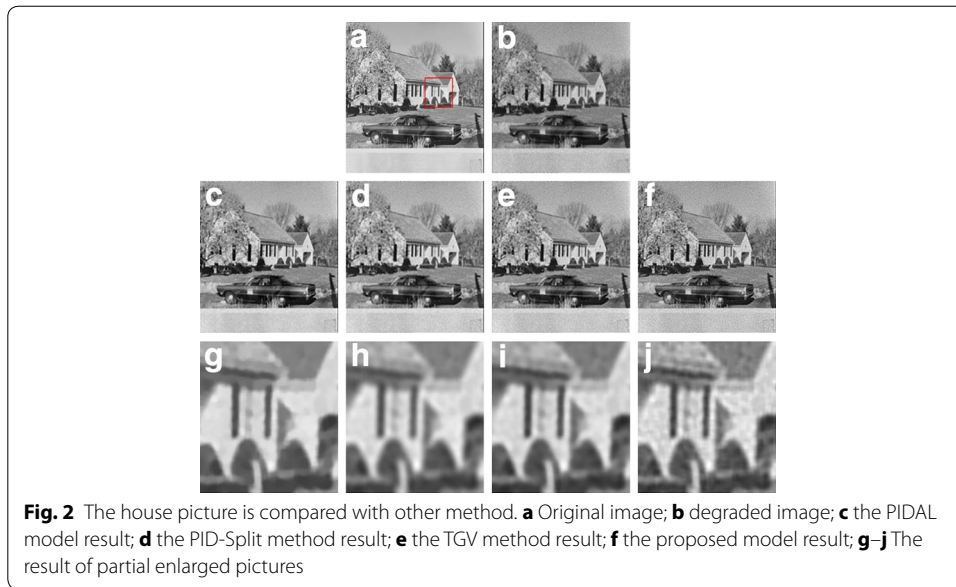


these pictures, we can see the proposed model have more advantages. In order to more effectively reflect the experiment result, Fig. 1g–j present the residual images refer to the difference of the original image and the restoration image. From these pictures, we can see that the proposed model can preserve more details than other methods. In the Table 1, the *SNR*, *PSNR*, *RelErr* and *SSIM* values of the restored images by the proposed model are better than other methods.

In second experiment, we use the image “House” with size  $(512 \times 512)$  in Fig. 2a, which contains a lot of edge details. We perform the blurring operation with radius 5 ( $psf = ones(5,5)/25$ ) on the original image and add the Poisson noise to the blurred data to generate the degraded image in Fig. 2b. As for parameter selection, we choose  $\beta = 200$  for the PIDAL algorithm,  $\beta = 20, \lambda = 0.00001$  for the PID-Split

**Table 1** Summarized all of the experiment restoration results

Method	SNR	PSNR	RelErr	SSIM
Test1				
PIDAL (Figueiredo and Bioucas-Dias 2010)	25.33	30.30	0.054	0.904
PID-Split (Liu and Huang 2012)	25.18	30.16	0.055	0.917
TGV	25.31	30.32	0.053	0.908
Proposed	25.48	30.45	0.053	0.922
Test2				
PIDAL (Figueiredo and Bioucas-Dias 2010)	21.17	25.03	0.087	0.828
PID-Split (Liu and Huang 2012)	21.38	25.36	0.084	0.837
TGV	21.24	25.10	0.086	0.835
Proposed	21.74	25.60	0.080	0.843
Test3				
PIDAL (Figueiredo and Bioucas-Dias 2010)	21.50	27.87	0.0841	0.811
PID-Split (Liu and Huang 2012)	21.49	27.86	0.0357	0.811
TGV	20.64	27.01	0.092	0.801
Proposed	21.01	27.23	0.0803	0.820



algorithm, set  $\beta = 450$ ,  $\alpha = [8, 10]$  in the TGV model. The proposed algorithm we set  $\beta = 75$ ,  $\lambda = 0.00001$ ,  $\alpha = [17, 13]$ . From Fig. 2c–f, we can see that the proposed model compared to the *PIDAL* method and *PID-Split* algorithms have better restoration results. In Fig. 2g–j, we have enlarged some details of the images, which can be clearly see the advantages of the proposed model for the recovery of edge details. The *SNR*, *RelRrr* and *SSIM* values in Table 1 showed that the proposed model have a better restoration result.

In order to further verify the validity of the new model, in third experiment, we use the image which contains a lot of edge details. We perform the blurring operation by a line motion blur. The point spread function for the linear motion blur is returns a filter to approximate, once convolved with an image, the linear motion of a camera by  $r$  pixels, with an angle of  $\theta$  degrees in a counter-clockwise direction. In this example,  $r = 2$  and  $\theta = 45$ , then add the Poisson noise to the blurred data to generate the degraded image in Fig. 3b. The parameters choose as the same as those in second experiment and also may be adjusted.

Finally, let us choose a human brain MR image of size  $240 \times 240$  as the test image. We zoom in a marked close-up region which is abundant in texture-like features to better visual comparison. We can clearly see that the produced textures by our proposed method are better quality than the other methods from Fig. 4.

## Conclusions

In this paper, we investigate the second-order total generalized variation with a quadratic regularization to deal with the Poissonian images restoration problem. The proposed model is solved efficiently by split Bregman iterative algorithm in this way the

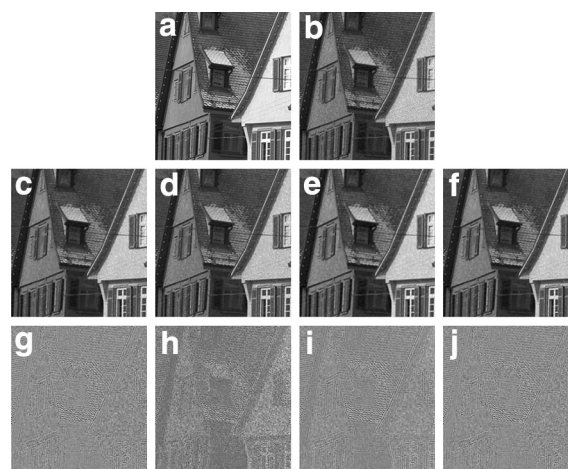


**Fig. 3** The third experiment. **a** Original image; **b** degraded image; **c** the PIDAL model result; **d** the PID-Split method result; **e** the TGV method result; **f** the proposed model result; **g–j** The residual images

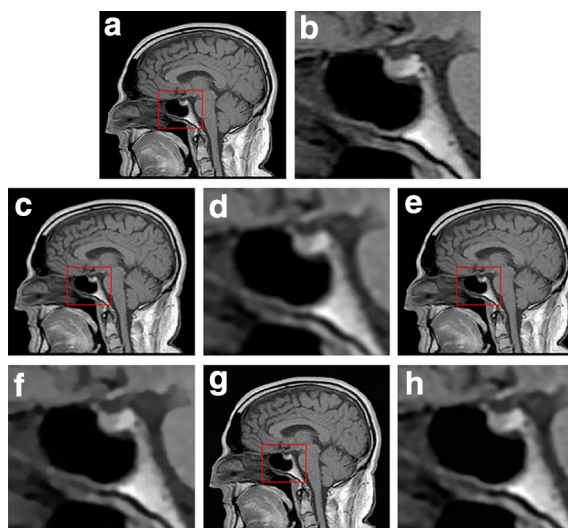


**Fig. 4** The fourth experiment. **a** Ground truth; **b** ground truth enlarge; **c** PID-Split method result; **d** PID-Split method enlarge; **e** PIDAL-Method result; **f** PIDAL-method enlarge; **g** Proposed method result; **h** proposed method enlarge

calculation speed is fast. Numerical results show that our proposed method is particularly advantageous for restoration the Poisson images in terms of *SNR*, *SSIM* and *RelErr* quality compared to other methods. In the model, the parameters selection is a difficult problem which needs further study.

#### Authors' contributions

All authors completed the paper together. All authors read and approved the final manuscript.

#### Acknowledgements

The authors would like to thank the anonymous referees for their helpful comments. This work was supported by National Natural Science foundation of China (51175443, 11101071).

#### Competing interests

The authors declare that they have no competing interests.

**Ethical approval**

This article does not contain any studies with human participants or animals performed by any of the authors.

Received: 25 April 2016 Accepted: 27 July 2016

Published online: 05 August 2016

**References**

- Bilal M, Mujtaba H, Jaffar MA (2015) Novel optimization framework to recover true image data. *Cogn Comput* 7(6):680–692
- Bredies K, Dong Y, Hintermiller M (2013) Spatially dependent regularization parameter selection in total generalized variation models for image restoration. *Int J Comput Math* 90(1):109–123
- Bredies K, Kunisch K, Pock T (2010) Total generalized variation. *SIAM J Imaging Sci* 3(3):492–526
- Bredies K, Valkonen T (2011) Inverse problems with second-order total generalized variation constraints. In: *Proceedings of SampTA 2011—9th International Conference on Sampling Theory and Applications*, Singapore
- Cai JF, Osher S, Shen Z (2009) Split Bregman methods and frame based image restoration. *Multiscale Model Simul* 8(2):337–369
- Chavent G, Kunisch K (1997) Regularization of linear least squares problems by total bounded variation. *ESAIM Control Optim Calc Var* 2:359–376
- Dey N, BlancFeraud L, Zimmer C et al (2006) Richardson–Lucy algorithm with total variation regularization for 3D confocal microscope deconvolution. *Microsc Res Tech* 69(4):260–266
- Figueiredo MAT, Bioucas-Dias JM (2010) Restoration of Poissonian images using alternating direction optimization. *IEEE Trans Image Process* 19(12):3133–3145
- Foi A, Alenius S, Trimeche M et al (2005) A spatially adaptive Poissonian image deblurring. In: *Proceedings of IEEE international conference on image processing*, vol 1, pp 925–928
- Goldstein T, Osher S (2009) The split Bregman method for L1-regularized problems. *SIAM J Imaging Sci* 2(2):323–343
- Guo W, Qin J, Yin W (2014) A new detail-preserving regularization scheme. *SIAM J Imaging Sci* 7(2):1309–1334
- Jia RQ, Zhao H, Zhao W (2009) Convergence analysis of the Bregman method for the variational model of image denoising. *Appl Comput Harmon Anal* 27(3):367–379
- Le T, Chartrand R, Asaki TJ (2007) A variational approach to reconstructing images corrupted by Poisson noise. *J Math Imaging Vis* 27(3):257–263
- Liu X, Huang L (2012) Total bounded variation-based Poissonian images recovery by split Bregman iteration. *Math Methods Appl Sci* 35(5):520–529
- Nagy JG, Palmer K, Perrone L (2004) Iterative methods for image deblurring: a Matlab object-oriented approach. *Numer Algorithms* 36(1):73–93
- Rudin LI, Osher S, Fatemi E (1992) Nonlinear total variation based noise removal algorithms. *Phys D Nonlinear Phenom* 60(1):259–268
- Sarder P, Nehorai A (2006) Deconvolution methods for 3-D fluorescence microscopy images. *IEEE Signal Process Mag* 23(3):32–45
- Sawatzky A, Brune C, Wubbeling F et al (2013) EM-TV methods for inverse problems with Poisson noise. In: *Lecture notes in mathematics*, vol 2090, pp 71–142
- Setzer S, Steidl G, Teuber T (2010) Deblurring Poissonian images by split Bregman techniques. *J Vis Commun Image Represent* 21(3):193–199
- Starck JL, Murtagh F (2007) *Astronomical image and data analysis*. Springer Science and Business Media, Berlin
- Wang Y, Yang J, Yin W, Zhang Y (2008) A new alternating minimization algorithm for total variation image reconstruction. *SIAM J Imaging Sci* 1:248–272
- Willetts RM, Nowak RD (2003) Platelets: a multiscale approach for recovering edges and surfaces in photon-limited medical imaging. *IEEE Trans Med Imaging* 22(3):332–350
- Zhao B, Zhang W, Ding H et al (2013) Non-blind image deblurring from a single image. *Cogn Comput* 5(1):3–12

**Submit your manuscript to a SpringerOpen<sup>®</sup> journal and benefit from:**

- Convenient online submission
- Rigorous peer review
- Immediate publication on acceptance
- Open access: articles freely available online
- High visibility within the field
- Retaining the copyright to your article

---

Submit your next manuscript at ► [springeropen.com](http://springeropen.com)

---